Efficient frequency doubling by a phase-compensated crystal in a semimonolithic cavity

Irit Juwiler and Ady Arie

In multiple-pass nonlinear frequency conversion devices, interacting waves may accumulate different phases, owing to dispersive elements in the system. Phase compensation is therefore necessary for efficient frequency conversion. We experimentally demonstrate phase compensation in a compact semimonolithic frequency-doubling cavity by using a periodically poled KTP crystal. The conversion efficiency of the crystal was found to decrease at high pump powers, owing to power-dependent thermal lensing. This experimental observation was supported by a theoretical calculation of the conversion efficiency in a cavity, considering the mismatch between the mode's thermally loaded and unloaded cavities. A design procedure was also presented to compensate for the thermal lensing effect. The highest conversion efficiency of 56.5%, corresponding to a second-harmonic power of 117.5 mW at 532 nm, was achieved with a cw Nd:YAG pump power of 208 mW.

OCIS codes: 190.0190, 190.2620, 230.4320.

1. Introduction

Resonant-cavity second-harmonic generation represents a powerful technique for the frequency doubling of low- and medium-power cw sources. A number of approaches based on singly and doubly resonant cavities for producing high-efficiency frequency doubling have been presented in the past.[1–5] Usually, the resonant cavities are in a ring or bow-tie configuration, since the light passes only in one direction through the doubling crystal. Standing-wave cavities can be more compact and potentially more efficient, owing to the reduction in the number of elements. However, in these cavities the second harmonic wave is generated both in the forward and in the backward directions, and one needs to add these two waves efficiently. Several methods have been proposed to solve this problem,[6–8] but at the expense of reducing the overall efficiency and compactness of the resonant cavity.

Recently we demonstrated a method to add coherently the forward- and backward-generated waves in a standing-wave cavity by using a wedged quasi-phase-matched frequency doubler in the cavity.[9] Translation of the doubler perpendicularly to the beam direction changes the thickness of the last domain of the crystal, thus allowing us to vary the phase between the forward- and backward-generated waves until constructive interference is obtained.[10] Whereas that work was performed with a cavity that contained two separate mirrors and a doubling crystal, in this work we perform another improvement in the compactness and robustness of the frequency-doubling method by eliminating one of the mirrors and using the output facet of the periodically poled KTP (PP-KTP) crystal as the second mirror of the standing-wave cavity. In this configuration we have one mirror less, which leads to a more compact, more robust, and cheaper design with a potentially higher conversion efficiency.

During the experiment we observed serious thermal lensing problems. The absorbed pump power in the crystal gives rise to thermal loading effects that are due to the temperature dependence of the refractive index and to the absorption coefficient. Hence the power transmission of the crystal as well as the parameters of the propagating laser beam are modified as a function of the incident pump power, and the operating characteristics of the resonator are inevitably affected. We have developed a model for calculating the effect of the thermal lensing on the overall efficiency of the resonant frequency doubler and have presented also a new design to compensate for the thermal lensing effect.

The authors are with the Department of Electrical Engineering-Physical Electronics, Tel Aviv University, Tel Aviv 69978, Israel. I. Juwiler's e-mail address is iritha@post.tau.ac.il.

Received 16 January 2003; revised manuscript received 16 June 2003.

0003-6935/03/367163-07$15.00/0

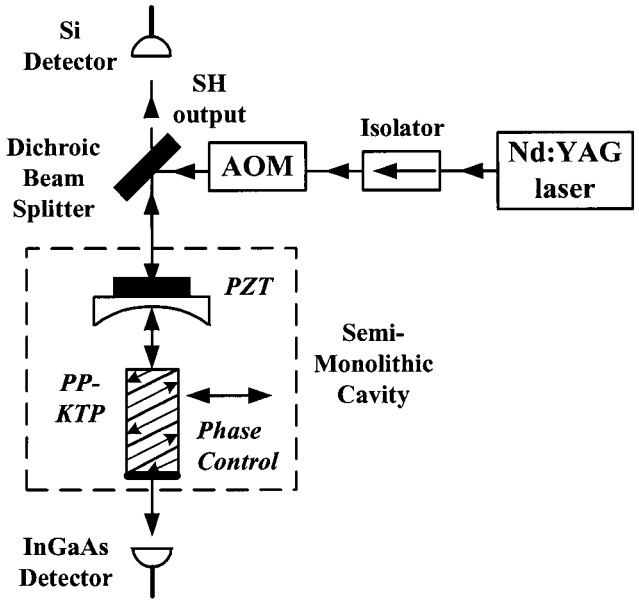

Fig. 1. Experimental setup for semimonolithic standing-wave resonant frequency doubling of Nd:YAG with a phase-compensated PP-KTP crystal. SH, second-harmonic; PZT, piezoelectric transducer; AOM, acousto-optic modulator.

The experimental setup is described in Section 2, and the frequency-doubling results for double-pass and standing-wave cavity are presented in Section 3. These results are compared with a theoretical model that is extended to include the effect of the thermal lensing in Section 4. A method for a compensating of the thermal lensing effect is proposed in Section 5. Section 6 contains a short discussion and a summary.

2. Experiment Setup

The KTP crystal[11] was a 20-mm-long, 2-mm-wide, and 0.5-mm-thick, periodically poled with a 9.0-μm period (equal to $2L_c$, where L_c is the coherence length for frequency doubling of 1064.4-nm light) by the technique of low-temperature electric-field poling.[12] The crystal faces were polished at a small angle with respect to the domain walls to permit phase correction by transverse movement. The input facet of the crystal was antireflection coated for the pump and the second-harmonic wavelengths, and the output facet of the crystal was highly reflection coated (HR-coated) for both wavelengths.

The experimental resonant frequency-doubling setup is shown in Fig. 1. Our pump source was a 1064.4-nm monolithic single-frequency Nd:YAG ring laser (Lightwave Electronics, Mountain View, California, Model 126-500). To overcome the feedback problems from the doubling cavity, the laser beam was passed through an isolator and an acousto-optic modulator. The waist radius of the laser beam inside the crystal should be 35.9 μm in order to have an optimal ratio of 2.84 between the crystal length and the confocal parameter[13] and thus to obtain high conversion efficiency. Note that since this is a double-pass configuration and the beam is focused to the rear end of the crystal, we used twice the crystal length (i.e., 4 cm) in the calculation. In this case the resonator length for optimal spatial mode matching should be ≈5.9 cm. The elliptic laser beam was focused by a positive thin lens of a focal length 150 mm to waist radii of 24 μm × 33 μm in the nonlinear crystal. The average focusing parameter in this case is 4.5, and the efficiency is reduced by less than 10% with respect to the optimal focusing.[13] The semimonolithic cavity included an input coupler with transmission coefficients of (5.63 ± 0.05)% and (92.0 ± 1.0)% at 1064 and 532 nm, respectively. The second cavity mirror was the HR-coated surface of the crystal, which reflected both the fundamental and the second-harmonic waves. The calculated waist radius of the laser beam inside the crystal was 25.4 μm. The radius of curvature of the mirror was 5.0 cm, and the physical distance between it and the HR-coated surface of the crystal was ≈5.9 cm. Fine control of the input coupler position (and thus the cavity length) was obtained by use of a piezoelectric transducer. The mode-matching efficiency to the cavity TEM_{00} mode was 88.6%.

The PP-KTP crystal was mounted upon a small copper block whose temperature was controlled to the optimal phase-matching temperature (≈56.9 °C). Note that the phase matching temperature of this crystal is higher by ~20 °C than PP-KTP crystals we have previously used, having the same poling period. We suspect that the change in the phase-matching temperature is due to different growth parameters of the KTP crystals. The crystal was positioned so that the focal point will be at the HR-coated surface. We controlled the phase difference between the reflected fundamental and the second-harmonic waves by changing the transverse position of the crystal by use of a mechanical micropositioner. The linear loss in the cavity was (1.48 ± 0.05)%, as determined from measurements of the finesse. The reflected light coming out of the cavity through the input coupler was mainly at the second harmonic, but a small portion of the fundamental frequency also leaked out. We used a dichroic splitter (95% transmission at 532 nm) to eliminate this residual fundamental power.

3. Experimental Results

We have first characterized the 20-mm-long PP-KTP doubling crystal in a double-pass configuration, as shown in Fig. 2. The inset shows the measurement of the second-harmonic power as a function of the crystal transverse position. Changing the transverse position by $\Delta x = 0.812$ mm changed the last domain width by a single coherence length. From these measurements we deduce that the angle between the crystal faces and the domain walls was $\approx L_c/\Delta x \approx 5.54$ mrad. We have then set the crystal's transverse position at the location that provided constructive interference between the forward- and the backward-generated waves, and took the remaining measurements in this location.

By measuring the second-harmonic power as a function of the pump power at the constructive inter-

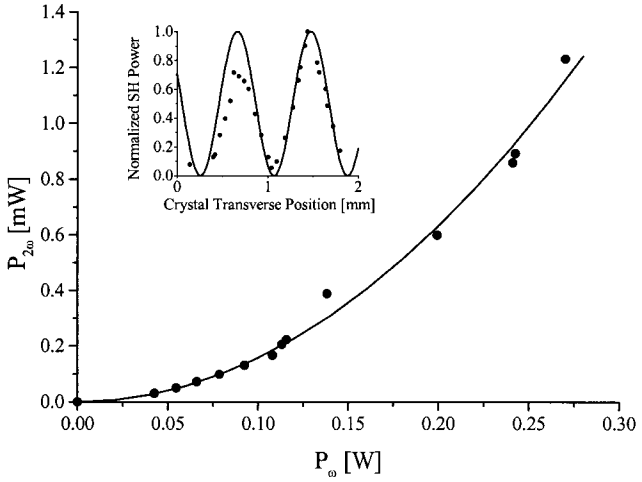

Fig. 2. Constructive-interference double-pass second-harmonic power as a function of the pump power. Inset: second-harmonic power as a function of the crystal transverse position. Solid curves, theoretical fits to the experimental data.

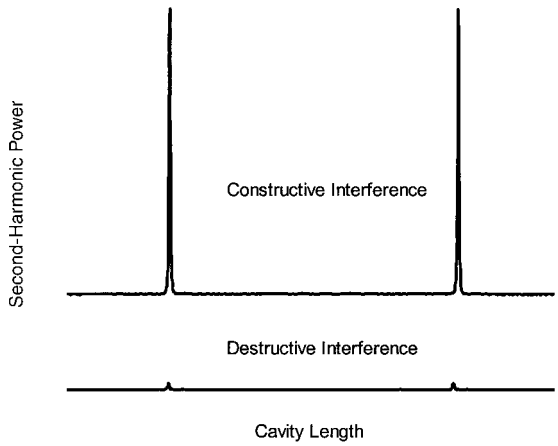

Fig. 4. Second-harmonic power when the cavity length was scanned, in the cases of constructive (top curve) or destructive (bottom curve) interference between the forward and the backward second-harmonic waves.

ference condition, we have deduced a conversion slope efficiency of 1.58% W^{-1}, which corresponds to a normalized conversion efficiency of 0.395% W^{-1} cm^{-1}. The value of the conversion efficiency is somewhat lower than that obtained in other PPKTP crystals,[9] due potentially to lower crystal and poling quality.

It should be noted that the double-pass efficiency differs in the case of reflection from a curved mirror or a flat mirror. The case in which the HR-coated surface of the crystal is a curved mirror that refocuses the beam is shown in Fig. 3(a). In this case, the beam is focused to the center of the crystal, and the conversion efficiency scales as $4L$, where L is the crystal length.[10] This is the configuration that was also used in Ref. 9. In the configuration used in this work, the HR-coated surface of the crystal acts as a plane mirror [see Fig. 3(b)], and the beam waist is therefore set to coincide with the HR-coated surface. In this case, the conversion efficiency scales as $2L$, which is lower by a factor of 2 with respect to the curved mirror configuration.

Phase compensation was also achieved in the semimonolithic standing-wave cavity. Two adjacent resonant peaks of the second-harmonic output power when the cavity length was scanned are shown in Fig. 4. The transverse location of the crystal was set for either constructive (top) or destructive (bottom) interference of the forward and backward second-harmonic waves.

When the pump power was increased, we have observed thermal-induced distortions in the first and second harmonic waves. These distortions are caused by an absorption of the pump and the second-harmonic waves, which generate a temperature gradient profile inside the crystal and therefore a thermal lens. Figure 5 shows three scans of the pump-power transmission versus cavity length, taken at three different incident pump powers where the transverse location of the crystal was set for con-

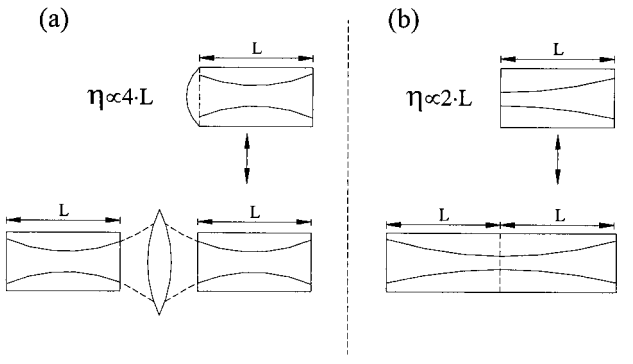

Fig. 3. Doubling crystal in double-pass configurations. (a) HR-coated surface of the crystal is a curved mirror. This is equivalent to having two crystals with a lens that refocuses the beam. (b) HR-coated surface of the crystal is a plane mirror. This is equivalent to having a crystal with length $2L$.

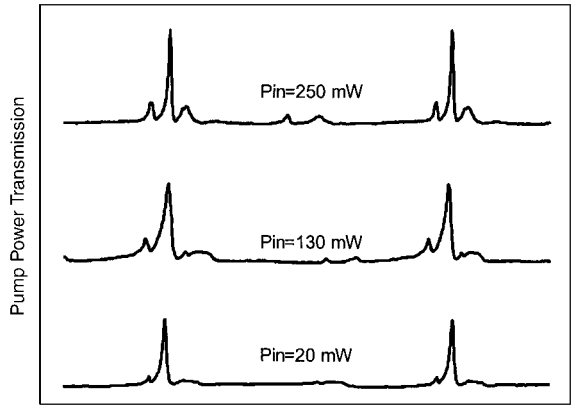

Fig. 5. Constructive-interference pump-power transmission versus cavity length at three different incident pump powers.

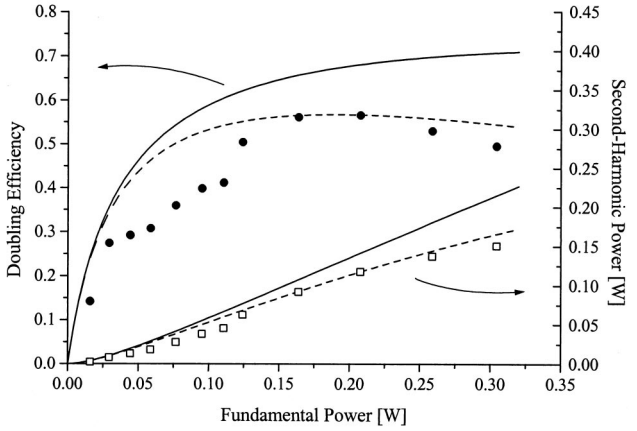

Fig. 6. Second-harmonic power and conversion efficiency as a function of fundamental power. Dotted and solid curves, theoretical results with and without thermal lensing, respectively.

structive interference. The comparison between the three scans, which were taken at low, medium and high pump power, shows clearly the thermal-induced distortions at high pump power. We have tried to partly compensate the thermal lensing by changing the location of the input mirror using a translation stage. However, we have not observed significant improvements.

Furthermore, whereas the conversion efficiency of the cavity increased with pump power at low power levels, when the pump power level reached ~200 mW, the conversion efficiency was clamped and even started to deteriorate as the pump power was increased further. Figure 6 shows the second-harmonic power and the doubling efficiency as a function of the pump power. The highest internal conversion efficiency of 56.5% (corresponding to green power of 117.5 mW) was obtained at a pump power of 208 mW. The pump power in front of the enhancement cavity was measured by a power meter with a germanium detector, whereas the second-harmonic power coming out through the input coupler of the cavity was measured by another power meter with a silicon detector. The accuracy of the power measurements for the pump and the second harmonic was 7%, and hence the accuracy in determining the efficiency was 10%.

4. Analysis of Experimental Results

We first compared the measured results with a theoretical calculation given by Polzik and Kimble[14] with parameters that were derived independently: transmission coefficient of the input coupler of 5.63%, round-trip conversion efficiency of 1.5% W^{-1} and loss of 1.48%.

$$\sqrt{\eta} = \frac{4T_1\sqrt{E_{NL}P_1}}{[2 - \sqrt{1 - T_1}(2 - L - \sqrt{\eta E_{NL}P_1})]^2}, \quad (1)$$

where $\eta \equiv P_2/P_1$ is the overall conversion efficiency, P_1 the fundamental input power, P_2 the second-harmonic output power, E_{NL} is the round-trip conversion efficiency, T_1 is the transmission coefficient of the input coupler, and L describes all linear losses in the cavity exclusive of T_1 (L and T_1 both refer to the fundamental field).

We found that the measured results are in a reasonable agreement with this theoretical calculation (shown as solid curves in Fig. 6) at low pump-power levels, but significant deviations are found at high pump-power levels. We assume that the deviations are due to the thermal lensing and therefore added this effect to the theoretical model: The power of the lens p [in diopters (D) or inverse meters] is given by[15]

$$P = \frac{1}{f_{th}} = \frac{\alpha(\mathrm{d}n/\mathrm{d}T)P^c}{\pi K_c}\int_{-L}^{L}\frac{\mathrm{d}z}{\omega^2(z)}, \quad (2)$$

where α (Ref. 16) (assumed to be 0.007 cm^{-1}) is the power absorption coefficient, $\mathrm{d}n/\mathrm{d}T$ (Ref. 17) (14.5×10^{-6}/°C) is the change of the refractive index with temperature, P^c is the intracavity power, K_c[18] [3W/(m °C)] is the thermal conductivity, L is the crystal length, and $\omega(z)$ is the waist of the pump power. Note that both the fundamental and the second-harmonic waves are absorbed in the crystal; hence we have assumed an absorption coefficient that is higher than derived only for the fundamental wave from the cavity finesse measurements. The intracavity power, P^c, was derived from[3]

$$P^c = \left(\frac{P_\omega \eta}{E_{NL}}\right)^{1/2}, \quad (3)$$

where P_ω is the pump power, η is the conversion efficiency, and E_{NL} is the round-trip conversion efficiency.

Since the circulating power is in the watt range, the thermal lens may be as small as ≈2 mm, which leads to a significant deviations from the unloaded ("cold") cavity. We have calculated the parameters of the cavity that includes the thermal lens. The measurements were taken during a dithering of the cavity length by use of the input cavity mirror, but only when the fundamental light is near the cavity resonance, the light is efficiently coupled into the cavity. Hence, the average input power coupled into the cavity was reduced by the cavity finesse (equal to ~83 at low conversion efficiency), and the effect on the thermal lensing was accordingly reduced. Since the beam is focused at the HR-coated surface of the crystal, we have assumed that the thermal lens is a thin lens located at this plane with an optical power given by Eq. (2). The combined effect of the reflection from the plane HR-coated surface and the thermal lens is therefore equivalent to that of a concave reflector. In this case, the mode of the cavity is a Gaussian beam having a waist with a different radius and location than that of the "cold" cavity. Since the input light beam is designed to match to the "cold" cavity parameters, matching losses will occur at high pump powers. These losses can be estimated by calculat-

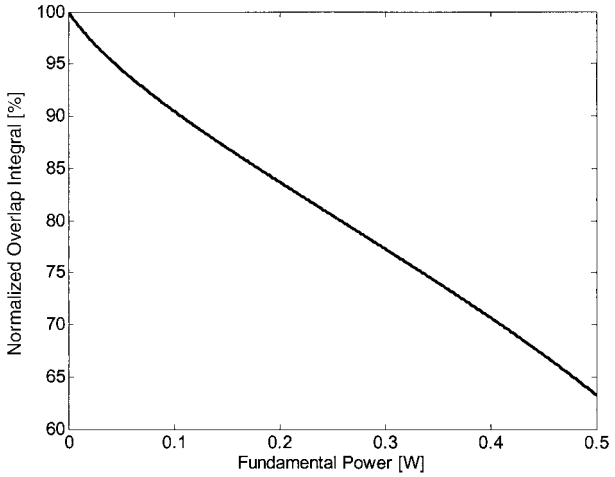

Fig. 7. Normalized overlap integral between the modes of the "cold" and thermally loaded cavities versus fundamental power.

ing the overlap integral between the modes of the "cold" and thermally loaded cavities:

$$\frac{\int_{-\infty}^{\infty}\int_{-\infty}^{\infty} E_1(x, y)E_2(x, y)\mathrm{d}x\mathrm{d}y}{\int_{-\infty}^{\infty}\int_{-\infty}^{\infty} |E_1(x, y)|^2\mathrm{d}x\mathrm{d}y}, \quad (4)$$

where $E_1(x, y)$ is the "cold" cavity field and $E_2(x, y)$ is the thermally loaded cavity field. The overlap integral is close to 100% at low pump power but is reduced to 77% at high pump powers; see Fig. 7. These matching losses of the input pump power will result in a reduced conversion efficiency. The "cold" cavity calculations were multiplied with the overlap integral. In Fig. 6, the dotted curves are the theoretical results with thermal lensing effects taken into account. The measured results are in a reasonable agreement with this theoretical calculation.

5. Compensating for Thermal Lensing

Dynamically stable cavities, which are relatively immune to variations in the power of a thermal lens inside the cavity, have been studied in the case of solid-state lasers by Magni[19,20] and by Hanna *et al.*[21] The design considerations of these cavities may also be applied to resonant frequency doubling cavities. In this section we outline a possible design that will enable us to partly overcome the effects of the thermal lensing described in Section 4. Magni[19,20] showed that through appropriate selection of spherical cavity mirrors and distances, a stable operating point is achieved in which the variations of the intracavity lens have a negligible effect on the beam parameters. Hanna *et al.*[21] proposed to use an intracavity telescope for overcoming thermal lensing. Whereas this method showed excellent results in solid-state laser applications, we believe that it is less suitable for nonlinear frequency-doubling applications, owing to the additional loss induced by the intracavity telescope. As shown in Eq. (1), the conversion efficiency is highly sensitive to the cavity losses. Hence, we have concentrated on designs that are based on an appropriate choice of mirrors and distances.[19,20]

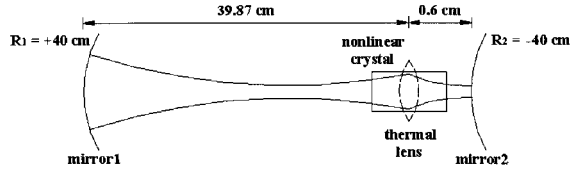

Fig. 8. Stable resonator accommodated for thermal lensing effects.

There are several possibilities for designing a dynamically stable cavity that includes a (thermal) lens and two spherical mirrors. There are four possible configurations to reach a dynamically stable cavity, two of them using a concave–concave cavity and two using concave–convex cavity. We have chosen a design based on a concave–convex cavity, since the cavity is shorter in this case. The cavity was designed for overcoming thermal lenses in the range 0.4–20 cm, in accordance with the thermal lenses obtained in our experiment. We have found that a stable design is reached if the radius of curvature of the cavity mirrors is twice the largest thermal lens (i.e., +40 cm and −40 cm for the concave and convex mirrors). The optimal physical distances between the first mirror and the lens and between the second mirror and the lens were found through numerical simulation to be 39.87 cm and 0.6 cm, respectively; see Fig. 8. The PP-KTP crystal length is 1 cm, and the spot size on the lens is ≈50.0 μm. As shown in Fig. 9, varying the focal length of the thermal lens in the range 0.4–20 cm has a negligible effect on the cavity waist size.

Another important design parameter for combating thermal lensing effects is appropriate selection of

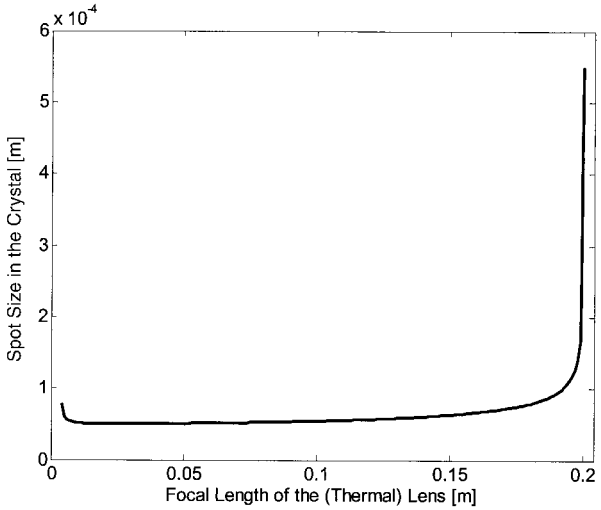

Fig. 9. Spot size in the crystal as a function of focal length of the (thermal) lens.

Table 1. Parameters that Determine the Sensitivity to Thermal Lensing for Several Commonly Used Nonlinear Crystals

Material	α (cm^{-1})	$\frac{dn}{dT}$ ($°C^{-1}$)	K_c ($W\ m^{-1}\ °C^{-1}$)	$\text{FOM} = \left\vert \frac{K_c}{\alpha \frac{dn}{dT}} \right\vert$ (W)
$LiNbO_3$	0.0019–0.0023[a]	99.5×10^{-6}[d]	4.6[a]	2.0×10^5–2.4×10^5
KTP	0.005–0.01[a]	14.5×10^{-6}[b]	3.0[c]	2.1×10^5–4.1×10^5
LBO[f]	0.00035[a]	-8.5×10^{-6}[a]	4.5[e]	1.5×10^7
BBO[f]	0.001–0.002[e]	-9.3×10^{-6}[a]	1.6[e]	8.6×10^5–1.7×10^6

[a]Ref. 16.
[b]Ref. 17.
[c]Ref. 18.
[d]Ref. 22.
[e]Ref. 23.
[f]LBO, lithium triborate; BBO, β-barium borate.

the nonlinear material. Table 1[16–18,22,23] shows the parameters of several commonly used nonlinear crystals. The resistance to thermal lensing effects is given by the figure of merit FOM, defined as

$$\text{FOM} = \left\vert \frac{K_c}{\alpha \frac{dn}{dT}} \right\vert$$

As can seen from Table 1, LBO has the highest resistance to thermal lensing. This may also explain the wide use of LBO in commercial high-average power-frequency-conversion applications. However, at low and moderate power, the much higher nonlinear coefficient of periodically poled ferroelectric materials enables us to reach higher conversion efficiencies.

6. Discussion and Summary

It is interesting to compare the semimonolithic cavity configuration with a standing-wave cavity configuration. In a semimonolithic cavity configuration the number of mirrors is smaller (one instead of two). This should reduce the loss level, and as a result higher conversion efficiency should be achieved. Furthermore, the system become much more compact. In a previous experiment we performed resonant frequency doubling of a Nd:YAG laser with a wedged PP-KTP crystal in a standing-wave cavity configuration.[9] Indeed, the smaller number of mirrors here (one instead of two) was among the reasons for the reduced loss level of 1.48% versus 2.0% in the standing-wave cavity. Furthermore, this time we also used a longer wedged PP-KTP crystal (20 mm long) in order to get higher conversion efficiency than is possible with a 10-mm-long crystal. However, higher conversion efficiency was not achieved, owing to serious thermal lensing problems. The thermal lensing strongly affected the operating characteristics of the semimonolithic cavity, thus leading to a reduced matching of the input wave to the cavity mode and as a result to a lower conversion efficiency.

In summary, we have demonstrated the use of a PP-KTP crystal with a small angle between the crystal faces and the domain walls to compensate for phase shifts between forward and backward second-harmonic waves in a semimonolithic cavity. High frequency-conversion efficiency was achieved at low input power levels in a relatively compact configuration. At higher pump powers, the efficiency was limited by thermal lensing effects. To compensate for the thermal lensing effect, a design procedure for a frequency doubling resonator with low sensitivity to focal length fluctuations has been proposed and analyzed.

Higher conversion efficiency can be obtained by using a semimonolithic cavity designed to accommodate thermal lensing effects.[24] The ideas proposed in Section 5 can be applied to semimonolithic cavities, e.g., by eliminating the air space between the crystal and input mirror R_2 in Fig. 8 and converting the input facet of the crystal into a curved facet. Further improvements in efficiency and size can be obtained by a monolithic cavity in which the input facet of the crystal acts as the input coupler. In this case, one may benefit from the thermal lensing: Without the thermal lens, the beam size of the mode supported by a nonlinear crystal with plane input and output facets is very large (the Rayleigh range of the beam should be much larger than the crystal length); thus the conversion efficiency will be low. The thermal lens enables us to support a tightly focused beam, which leads to a significantly higher conversion efficiency.

References

1. A. Ashkin, G. D. Boyd, and J. M. Dziedzic, "Resonant optical second-harmonic generation and mixing," IEEE J. Quantum Electron. **QE-2,** 109–124 (1966).
2. W. J. Kozlovsky, C. D. Nabors, and R. L. Byer, "Second-harmonic generation of a continuous-wave diode-pumped Nd:YAG laser using an externally resonant cavity," Opt. Lett. **12,** 1014–1016 (1987).
3. W. J. Kozlovsky, C. D. Nabors, and R. L. Byer, "Efficient second harmonic generation of a diode-laser-pumped cw Nd:YAG laser using monolithic MgO:$LiNbO_3$ external resonant cavities," IEEE J. Quantum Electron. **QE-24,** 913–919 (1988).
4. D. H. Jundt, G. A. Magel, M. M. Fejer, and R. L. Byer, "Periodically poled $LiNbO_3$ for high-efficiency second-harmonic generation," Appl. Phys. Lett. **59,** 2657–2659 (1991).

5. Z. Y. Ou and H. J. Kimble, "Enhanced conversion efficiency for harmonic generation with double resonance," Opt. Lett. **18,** 1053–1055 (1993).
6. R. Paschotta, P. Kurz, R. Henking, S. Schiller, and J. Mlynek, "82% Efficient continuous-wave frequency doubling of 1.06 μm with a monolithic MgO:$LiNbO_3$ resonator," Opt. Lett. **19,** 1325–1327 (1994).
7. C. Zimmermann, R. Kallenbach, T. W. Hansch, and J. Sandberg, "Doubly-resonant second-harmonic generation in β-barium-borate," Opt. Commun. **71,** 229–234 (1989).
8. J. M. Yarborough, J. Falk, and C. B. Hitz, "Enhancement of optical second harmonic generation by utilizing the dispersion of air," Appl. Phys. Lett. **18,** 70–73 (1971).
9. I. Juwiler, A. Arie, A. Skliar, and G. Rosenman, "Efficiency quasi-phase-matched frequency doubling with phase compensation by a wedged crystal in a standing-wave external cavity," Opt. Lett. **24,** 1236–1238 (1999).
10. G. Imeshev, M. Proctor, and M. M. Fejer, "Phase correction in double-pass quasi-phase-matched second-harmonic generation with a wedged crystal," Opt. Lett. **23,** 165–167 (1998).
11. Raicol Crystals, Ltd., P. O. Box 2753, Industrial Zone, Yehud 56217, Israel.
12. G. Rosenman, A. Skliar, D. Eger, M. Oron, and M. Katz, "Low temperature periodic electrical poling of flux-grown $KTiOPO_4$ and isomorphic crystals," Appl. Phys. Lett. **73,** 3650–3652 (1998).
13. G. D. Boyd and D. A. Kleinman, "Parametric interaction of focused Gaussian light beams," J. Appl. Phys. **39,** 3597–3639 (1968).
14. E. S. Polzik and H. J. Kimble, "Frequency doubling with $KNbO_3$ in an external cavity," Opt. Lett. **16,** 1400–1402 (1991).
15. A. Douillet, J. J. Zondy, A. Yelisseyev, S. Lobanov, and L. Isaenko, "Stability and frequency tuning of thermally loaded continuous-wave $AgGaS_2$ optical parametric oscillators," J. Opt. Soc. Am. B **16,** 1481–1498 (1999).
16. V. G. Dimitriev, G. G. Gurzadyan, and D. N. Nikogosyan, *Handbook of Nonlinear Optical Crystals*, 2nd ed. (Springer, New York, 1997).
17. W. Wiechmann, S. Kubota, T. Fukui, and H. Masuda, "Refractive-index temperature derivatives of potassium titanyl phosphate," Opt. Lett. **18,** 1208–1210 (1993).
18. J. D. Bierlein and H. Vanherzeele, "Potassium titanyl phosphate: properties and new applications," J. Opt. Soc. Am. B **6,** 622–633 (1989).
19. V. Magni, "Resonators for solid-state lasers with large-volume fundamental mode and high alignment stability," Appl. Opt. **25,** 107–117 (1986).
20. V. Magni, "Resonators for solid-state lasers with large-volume fundamental mode and high alignment stability," Appl. Opt. **25,** 107–117 (1986).
21. D. C. Hanna, C. G. Sawyers, and M. A. Yuratich, "Telescopic resonators for large-volume TEM_{00}-mode operation," Opt. Quantum Electron. **13,** 493–507 (1981).
22. D. H. Jundt, "Temperature-dependent Sellmeier equation for the index of refraction, n_e, in congruent lithium niobate," Opt. Lett. **22,** 1553–1555 (1997).
23. http://www.clevelandcrystals.com/BBOLBO.shtml.
24. A. E. Siegman, *Lasers* (University Science, Mill Valley, Calif., 1986), pp. 842–845.